Volume 1 | Number 1 | Jan 2013 | Pages 1–100

ChemComm

Chemical Communications
www.rsc.org/chemcomm

ROYAL SOCIETY OF CHEMISTRY

This is an *Accepted Manuscript*, which has been through the Royal Society of Chemistry peer review process and has been accepted for publication.

Accepted Manuscripts are published online shortly after acceptance, before technical editing, formatting and proof reading. Using this free service, authors can make their results available to the community, in citable form, before we publish the edited article. We will replace this *Accepted Manuscript* with the edited and formatted *Advance Article* as soon as it is available.

You can find more information about *Accepted Manuscripts* in the **Information for Authors**.

Please note that technical editing may introduce minor changes to the text and/or graphics, which may alter content. The journal's standard **Terms & Conditions** and the **Ethical guidelines** still apply. In no event shall the Royal Society of Chemistry be held responsible for any errors or omissions in this *Accepted Manuscript* or any consequences arising from the use of any information it contains.

Journal Name

Dynamic Article Links ►

ARTICLE TYPE

Facial Synthesis of Hydrophilic Multi-colour and Upconversion Photoluminescent Mesoporous Carbon Nanoparticles for Bioapplications

Qinglu Kong[a], Lingxia Zhang[a], Jianan Liu[a], Meiying Wu[a], Yu Chen[a], Jingwei Feng[a], Jianlin Shi[a]*

Hydrophilic mesoporous carbon nanoparticles (MCNs) have been synthesized by an extremely facile precursor carbonization-in-hot solvent route. The synthesized MCNs
10 **show well-defined particle and pore size distribution around 100 nm and 2.7 nm, respectively, and multicolor and upconversion photoluminescence, which endow the MCNs with multicolor/upconversion bioimaging and drug delivery properties.**

15   Mesoporous nanoparticles have attracted ever greater attention recently owing to their open-framework structure, large surface area and well-defined mesoporosity, which make them greatly interesting and potentially useful in many fields such as adsorption[1,2], cellular delivery[3-6], energy storage[7-9], drug release
20 and delivery[10-15], and catalysis[16-18]. Similar to mesoporous silica nanoparticles (MSNs), mesoporous carbon nanoparticles (MCNs) are nontoxic and biocompatible[19]. However, unlike other drug delivery carriers such as MSNs[20,21], gold nanoparticles[22-24] or iron oxide[25-27], the biomedical property and applications of MCNs
25 have been much less explored most probably due to the difficulties in fabricating hydrophilic, nanosized and highly dispersed MCNs which are the premises for the biological applications such as bioimaging, and also to the lack of functionalities of traditionally synthesized MCNs. Conventional
30 approaches for the mesoporous carbon synthesis include hard-templating[28-30] and soft-templating methods[31], which usually involves the use of toxic surfactant and time-consuming multi-steps. More importantly, the synthesized MCNs frequently suffer from the over-large size, unstable dispersity in aqueous solutions
35 and/or strong aggregation among particles.

  Herein we report an especially facile approach for synthesizing nanosized MCNs, which, though aggregated to a limited extent, are of high dispersity in aqueous solutions and well-defined size distribution at around 100 nm without
40 employing any toxic surfactant. More importantly, in addition to its defined mesoporosity, such MCNs exhibit strong and stable multicolor photoluminescent property including upconversion photoluminescence, which endows the synthesized MCNs with promising features for drug delivery and fluorescent bioimaging.

45   MCNs were synthesized using a very simple route of precursor carbonization in hot organic solvent (denoted as PC-*in*-HS), in which only one step, citric solution as organic carbon source being quickly added into 1-octadecane at 240°C, is necessary. In about five minutes MCNs can be obtained without the need of

50 any further treatment, which is in great contrast with reported time-consuming and complicated fabrication methods such as template replications[28-30]. Such synthesized MCNs exhibit satisfactory biocompatibility and high photoluminescence efficiencies of 37%, and have been demonstrated to be highly
55 applicable for the photoluminescent imaging of Hela cells and anticancer drug (Doxorubicin, DOX) delivery to kill these cancer cells.
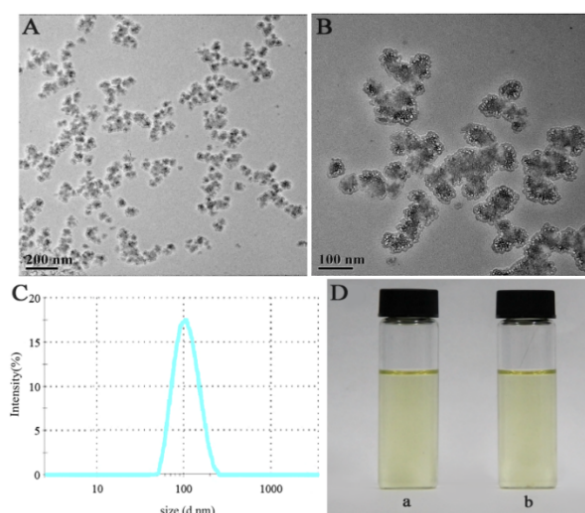
Figure 1. A) TEM image of MCNs prepared by a PC-*in*-HS
60 (precursor carbonization in hot solvent) approach at 240°C; B) High magnification TEM image of the synthesized MCNs; C) DLS size distribution of MCNs showing the well-defined size distribution though the primary particles are a little aggregated; D) The photograph of MCNs in water in 1 day (a) and 7 months (b).

65   The detailed PC-*in*-HS synthesis procedure is given in experimental section. The synthesis produces a transparent yellow dispersion solution of the mesoporous carbon nanoparticles in 1-octadecane solvent. The TEM image (Figure 1A) of MCNs shows that the MCNs have a primary particle size
70 of ca. 30-50nm, however, these particles are aggregated with each other to a certain extent, most probably due to the very quick decomposition/carbonization of the carbon source during synthesis. Fortunately, the dynamic light scattering (DLS, Figure 1C) reveals the high dispersity of the MCNs of ca.104 nm in
75 aggregate diameter with the maximum size not larger than 230

nm. The high dispersity of the synthesized MCNs is further visualized in Figure 1D, which gives the synthesized MCNs solution after standing for 7 months in water or in phosphate-buffered saline (PBS, pH7.4, not shown), no precipitation of large particles can be found. More interestingly, the high magnification TEM image in Figure 1B reveals that the MCNs have a porous structure. The mesoporous structure of the MCNs was further confirmed by N_2 sorption isotherms (Figure S3A in the Supporting Information), which shows typical pseudo-type-IV curve with clear capillary condensation steps. The pore size distribution can be calculated to be 2.7 nm from the adsorption branch based on density functional theory mode. The BET surface area and pore volume were calculated to be 864 m^2/g and 0.91 cm^3/g, respectively.
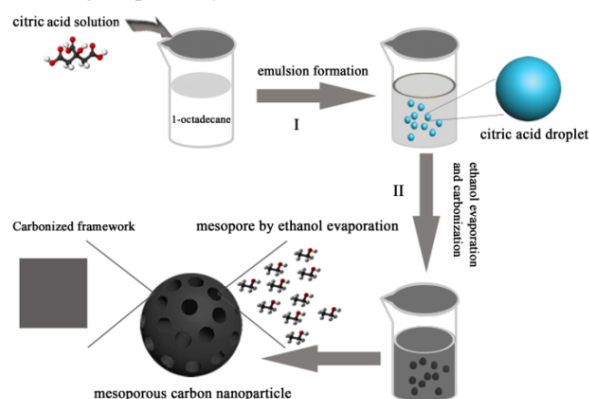
Scheme1. Schematic illustration of the formation processes of MCNs. I: citric acid droplet formation in hot 1-octadecane solvent at 240 °C immediately after the citric acid was added into the solvent; II: ethanol evaporation and carbonization of citric acid in the hot solvent.

Based on the above observations, we propose a quick carbonization mechanism to depict the formation of MCNs, as illustrated in Scheme 1. First, citric acid solution in ethanol as the carbon source was dispersed into emulsion droplets in 1-octadecene at 240°C when added into the hot solvent due to the hydrophilic-hydrophobic interaction between the hydrophilic citric solution and the highly hydrophobic solvent, forming a water-in-oil micro-emulsion. Immediately after the addition and emulsion formation, ethanol which has a low boiling point of 175°C in the droplet will quickly evaporate in the high temperature solvent, and escape from the droplets and the emulsion system, leading to the instant and remarkable shrinkage of the droplets. Afterwards, the droplets will be further heated immediately by the hot medium, leading to the decomposition of citric acid when the droplet temperature is above the decomposition temperature (175 °C) of citric acid. During the decomposition, citric acid will actually undergo carbonization due to absence of oxidants in the solvent, and the carbonization product serves as the framework of the fabricated MCNs, while the volume shrinkage during carbonization and ethanol evaporation as well result in nanosized particulate product, and in the meantime, leaves extensive mesoporous structure in the produced MCNs. The instant heating above the decomposition temperature of citric acid droplets in the solvent medium is the key to the formation of MCNs from the citric acid droplets. However, it is worthy to point out that, as the processes of ethanol evaporation and citric acid decomposition in hot solvent are so quick, fine control over the process might be difficult, so such obtained MCNs show a certain extent of aggregation. Nevertheless, the final MCNs show extremely high and stable

dispersion in water which enable the fabricated MCNs applicable in biomedicine.
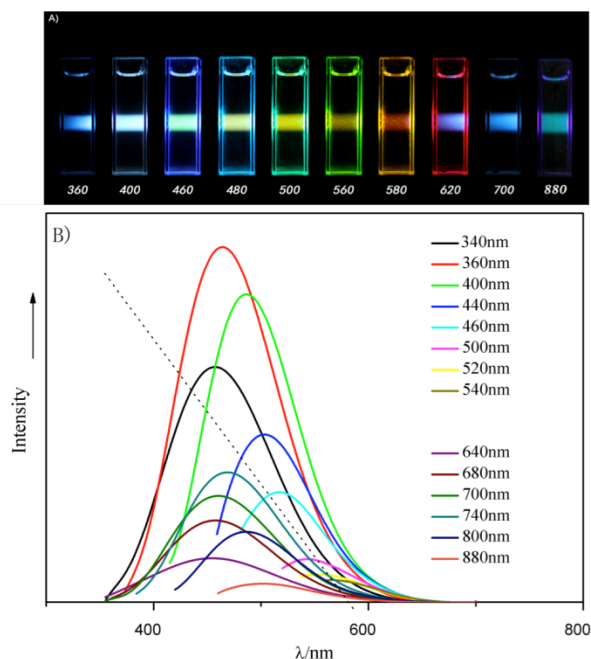
Figure 2. Photographs (A) and photoluminescent spectra (B) of as synthesized MCNs in water under the excitations of varied wavelengths of light as indicated. Curves above the dashed line in the figure are conventional downconversion photoluminescent spectra, and the relatively bold ones under the dashed line are the upconversion photoluminescent spectra.

The optical behavior of the synthesized MCNs is similar to their carbon dots counter-parts reported[32], both of which show multi-color and wavelength-dependent fluorescent emissions under excitations of varied wavelengths. In particular, the MCNs exhibit strong green to blue photoluminescence under excitation at 360 nm and 700 nm (see the photograph in Figure 2B), which means the MCNs display both the regular downconversion and upconversion light emission properties. To ensure the facticity of upconversion luminescence, optical filters with varied cut-off wavelengths were applied to stop any light incidence shorter than the cut-off wavelengths reaching the materials. As shown in Figure 2, the luminescence spectra of the MCNs under excitation of varied wavelengths are relatively broad, ranging from 425 nm to 580 nm, dependent on the excitation wavelengths. It should be noted that the upcoversion photoluminescence of the MCNs under the excitation by near infrared light (NIR) above 600 nm will greatly favor their future applications in solar cells and phototherapy. As shown in Figure S7, we speculate that the upconversion photoluminescence of MCNs may be attributed to the multiphoton active process, similar to the widely accepted fluorescent mechanism[33], known as anti-Stokes photoluminescence, in which when excitation energy is resonant with the transition from ground level G to excited metastable level E1, light absorption occurs. Immediately a second photon will be absorbed that promotes MCNs from excited metastable E1 to higher state E2. Thus the successive absorption of pump photons results in the emission of shorter wavelength photon compared with the excitation wavelength. The downconversion photoluminescence property can be regularly attributed to the higher excitation energy of photons promoting MCNs from ground level G to higher state E2, than that of the emission

photons due to the energy dissipation. The quantum yield was calculated to be ca.37% under 360nm excitation, which is higher than most reported carbon dots[34-40] and comparable with semiconductor quantum dots such as CdSe/ZnS QDs[41,42].

5　Furthermore, the photoluminescence of the synthesized MCNs are stable, no significant changes of the photoluminescence under 360 nm to 880 nm excitations have been found after being kept for 1 year at room temperature, which endows them with excellent sustained applicability.

10
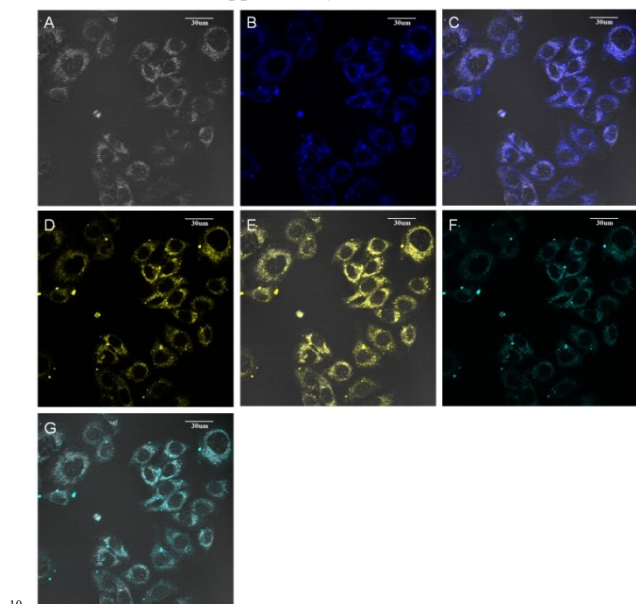
Figure 3. (A) Confocal microscopic images of Hela cells labeled with the mesoporous carbon nanospheres, which are incubated for 24h at 37°C in DMEM containing 0.1mg/mL of the MCNs. B,D,F): The images excited under λ_{ex}= 340nm (B) and detected

15　with 425-475 nm long-pass filter, under λ_{ex} = 488 nm (D) and detected with 520-560 nm and under λ_{ex} = 637 nm (F) and detected with 425-475 nm long-pass filter; C, E, G): the merged images. All scale bars are 30μm.

Laser scanning confocal microscopy images demonstrate that

20　such MCNs are excellent fluorescent bioimaging agents with satisfactory biocompatibility. Figure 3B shows the Hela cells incubated and labeled with the MCNs for 24h, remarkable intracellular fluorescence can be observed in the confocal image, revealing that the MCNs can be easily internalized within and

25　label the Hela cells. The image (Figure 3A) and over-lapped fluorescence images (Figure 3C) further demonstrate that the MCNs have accumulated and distributed uniformly in the whole regions of the cytosol, which indicates that the MCNs can be well endocytosized by living Hela cells, favoring the fluorescent

30　imaging of the whole cells and drug delivery into cytoplasm. The laser confocal fluorescence images also demonstrate the excellent photostability of the MCNs without any visible blinking and/or photo-bleaching. To further investigate the bioimaging application under varied excitations, we also used light of longer

35　wavelengths, as can be seen from Figure 3(D, E) and 3 (F, G). Especially, upconversion photoluminescence bioimaging has been achieved under the 637 nm excitation, which exhibits high quality green images for cell labeling (Figure 3(F, G)).

To further examine the drug delivery of the MCNs,

40　Doxorubicin, a widely used anticancer drug, was loaded into MCNs. The loading efficiency of DOX was measured to be as high as 76.1% while the loading capacity was calculated to be

43.6μgDOX mg^{-1}, due to the high BET surface and pore volume of the prepared MCNs. Figure 4(A) shows the DOX release

45　profile of the DOX-loaded MCNs in PBS at 37°C, which shows no initial burst release and sustained release behaviour for no shorter than 50 h. 56.3% DOX is released in the initial 10 h as compared with 98.2% DOX release from dialysis bag, and finally, about 72% DOX is released at the end of the release experiments

50　in 50 h. The mesostructure of relatively small pore diameter should be responsible for the sustained release of DOX molecules from the mesopore channels of MCNs.
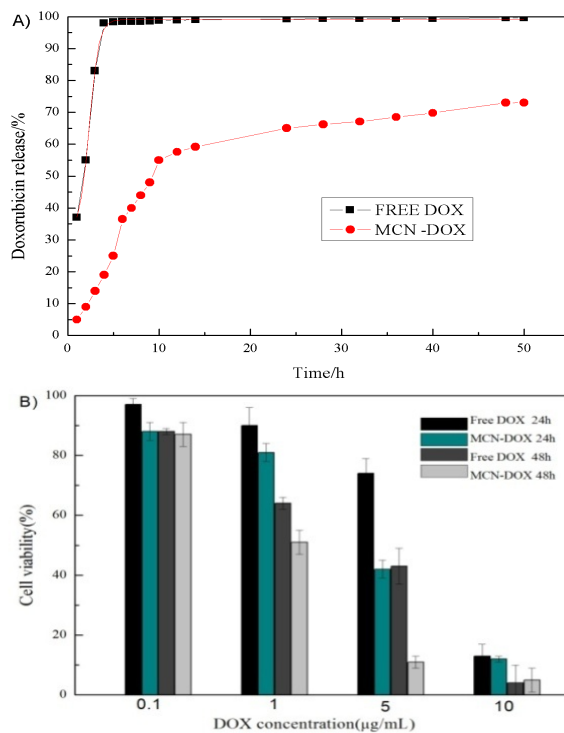
Figure 4. A) Release profiles of DOX from DOX-loaded MCNs

55　and free DOX from dialysis bag in PBS at 37°C. B) Cell viabilities of free DOX, DOX-loaded MCNs at 0.1, 1, 5and 10 μg/mL.

We studied the cytotoxic effect of the DOX-loaded MCNs

60　against Hela cell to verify whether the released DOX was pharmacologically active. As demonstrated in Figure 4(B), similar to free drug, the cytotoxicity of the DOX-loaded MCNs shows a dose-dependent increase at increased DOX concentrations, and it should be pointed out that the DOX-loaded

65　MCNs exhibit significantly higher cytotoxicity than free DOX, especially at relatively low DOX concentrations, such as at not higher than 5 μg/mL. This may be attributed to the easier uptake of the DOX-loaded MCNs *via* endocytosis by Hela cells as compared to the passive diffusion of free DOX molecules, which

70　is believed to be highly important in minimizing the toxic side effect of free drugs to normal tissues/cells. In all, the synthesized MCNs with extensive mesoporosity, high and stable dispersity and well-defined particle and pore sizes can serve as effective carriers for anticancer drug delivery for efficiently inducing

75　cancer cell death at rather low drug dosages.

In conclusion, we have developed an extremely facile method of synthesizing multicolor and upconversion photoluminescent mesoporous carbon nanoparticles (MCNs) by quickly adding carbon precursor (citric acid) into hot organic solvent (1-

80　octadecane) without using any surfactant. The synthesized MCNs

are free from any toxic metal ions which are present in most upconversion nanoparticles, exhibit defined mesoporosity of 2-3 nm in mesopore diameter and well-defined particle size distribution at around 100 nm though the primary particles are aggregated to a limited extent. Such synthesized MCNs are featured with remarkable stable multicolor and upconversion photoluminescence property with a high quantum yield of ca.37%, which is validated by using optical filters with varied cut-off wavelengths in the measurements. The MCNs can be well-uptaken by cancer cells and therefore can visibly label the cells under the excitations of varied wavelengths from ultraviolet to NIR. Moreover, the anticancer drug loading and delivery of MCNs are verified which show much enhanced cytotoxicity to cancer cells than the free drug.

Notes and references

a State Key Laboratory of High Performance Ceramic and Superfine Microstructure, Shanghai Institute of Ceramics, Chinese Academy of Sciences, Shanghai, 200050, P. R. China. Fax: +86-21-52413122; Tel: +86-21-52412712; E-mail: jlshi@mail.sic.ac.cn

† Electronic Supplementary Information (ESI) available: Experimental Section, detailed description of the MCNs including the synthesis procedures, materials characterization, along with supplementary figures. See DOI:10.1039/b000000x/

(1) Tian, R.; Zhang, H.; Ye, M.; Jiang, X.; Hu, L.; Li, X.; Bao, X.; Zou, H. *Angewandte Chemie International Edition* **2007**, *46*, 962.

(2) Ariga, K.; Vinu, A.; Miyahara, M.; Hill, J. P.; Mori, T. *Journal of the American Chemical Society* **2007**, *129*, 11022.

(3) Zhang, X.; Li, Y.; Cao, C. *Journal of Materials Chemistry* **2012**, *22*, 13918.

(4) Ma, M.; Chen, H.; Chen, Y.; Wang, X.; Chen, F.; Cui, X.; Shi, J. *Biomaterials* **2012**, *33*, 989.

(5) Liu, J.-n.; Bu, W.; Pan, L.-m.; Zhang, S.; Chen, F.; Zhou, L.; Zhao, K.-l.; Peng, W.; Shi, J. *Biomaterials* **2012**, *33*, 7282.

(6) Gu, J.; Su, S.; Li, Y.; He, Q.; Shi, J. *Chemical Communications* **2011**, *47*, 2101.

(7) Chang, H.; Joo, S. H.; Pak, C. *Journal of Materials Chemistry* **2007**, *17*, 3078.

(8) Liu, H.-J.; Cui, W.-J.; Jin, L.-H.; Wang, C.-X.; Xia, Y.-Y. *Journal of Materials Chemistry* **2009**, *19*, 3661.

(9) Yuan, Z.-Y.; Su, B.-L. *Journal of Materials Chemistry* **2006**, *16*, 663.

(10) Vivero-Escoto, J. L.; Slowing, I. I.; Trewyn, B. G.; Lin, V. S. Y. *Small* **2010**, *6*, 1952.

(11) Yuan, L.; Tang, Q.; Yang, D.; Zhang, J. Z.; Zhang, F.; Hu, J. *The Journal of Physical Chemistry C* **2011**, *115*, 9926.

(12) Gao, Y.; Chen, Y.; Ji, X.; He, X.; Yin, Q.; Zhang, Z.; Shi, J.; Li, Y. ACS Nano 2011, 5, 9788.

(13) Gai, S.; Yang, P.; Li, C.; Wang, W.; Dai, Y.; Niu, N.; Lin, J. Advanced Functional Materials 2010, 20, 1166.

(14) Slowing, I.; Viveroescoto, J.; Wu, C.; Lin, V. Advanced Drug Delivery Reviews 2008, 60, 1278.

(15) Zhao, Y.; Trewyn, B. G.; Slowing, I. I.; Lin, V. S. Y. Journal of the American Chemical Society 2009, 131, 8398.

(16) Clacens, J. M.; Pouilloux, Y.; Barrault, J. *Applied Catalysis A: General* **2002**, *227*, 181.

(17) Vasylyev, M. V.; Neumann, R. *Journal of the American Chemical Society* **2003**, *126*, 884.

(18) Eimer, G.; Casuscelli, S.; Ghione, G.; Crivello, M.; Herrero, E. *Applied Catalysis A: General* **2006**, *298*, 232.

(19) Kim, T.-W.; Chung, P.-W.; Slowing, I. I.; Tsunoda, M.; Yeung, E. S.; Lin, V. S. Y. *Nano Letters* **2008**, *8*, 3724.

(20) He, Q.; Shi, J. *Journal of Materials Chemistry* **2011**, *21*, 5845.

(21) Chen, Y.; Chen, H.; Shi, J. *Advanced Materials* **2013**, *25*, 3144.

(22) Niikura, K.; Iyo, N.; Higuchi, T.; Nishio, T.; Jinnai, H.; Fujitani, N.; Ijiro, K. *Journal of the American Chemical Society* **2012**, *134*, 7632.

(23) Milligan, W. O.; Morriss, R. H. *Journal of the American Chemical Society* **1964**, *86*, 3461.

(24) Millstone, J. E.; Park, S.; Shuford, K. L.; Qin, L.; Schatz, G. C.; Mirkin, C. A. *Journal of the American Chemical Society* **2005**, *127*, 5312.

(25) Weissleder, R.; Elizondo, G.; Wittenberg, J.; Rabito, C. A.; Bengele, H. H.; Josephson, L. *Radiology* **1990**, *175*, 489.

(26) Zhang, H.; Ming, H.; Lian, S.; Huang, H.; Li, H.; Zhang, L.; Liu, Y.; Kang, Z.; Lee, S.-T. *Dalton Transactions* **2011**, *40*, 10822.

(27) Jeong, U.; Teng, X.; Wang, Y.; Yang, H.; Xia, Y. *Advanced Materials* **2007**, *19*, 33.

(28) Ren, J.; Ding, J.; Chan, K.-Y.; Wang, H. *Chemistry of Materials* **2007**, *19*, 2786.

(29) Fuertes, A. B. *Journal of Materials Chemistry* **2003**, *13*, 3085.

(30) Yan, X.; Song, H.; Chen, X. *Journal of Materials Chemistry* **2009**, *19*, 4491.

(31) Fang, Y.; Gu, D.; Zou, Y.; Wu, Z.; Li, F.; Che, R.; Deng, Y.; Tu, B.; Zhao, D. *Angewandte Chemie International Edition* **2010**, *49*, 7987.

(32) Liu, R.; Wu, D.; Liu, S.; Koynov, K.; Knoll, W.; Li, Q. *Angewandte Chemie* **2009**, *121*, 4668.

(33) Cao, L.; Wang, X.; Meziani, M. J.; Lu, F.; Wang, H.; Luo, P. G.; Lin, Y.; Harruff, B. A.; Veca, L. M.; Murray, D.; Xie, S.-Y.; Sun, Y.-P. *Journal of the American Chemical Society* **2007**, *129*, 11318.

(34) Peng, H.; Travas-Sejdic, J. *Chemistry of Materials* **2009**, *21*, 5563.

(35) Liu, H.; Ye, T.; Mao, C. *Angewandte Chemie International Edition* **2007**, *46*, 6473.

(36) Bourlinos, A. B.; Stassinopoulos, A.; Anglos, D.; Zboril, R.; Georgakilas, V.; Giannelis, E. P. *Chemistry of Materials* **2008**, *20*, 4539.

(37) Bourlinos, A. B.; Stassinopoulos, A.; Anglos, D.; Zboril, R.; Karakassides, M.; Giannelis, E. P. *Small* **2008**, *4*, 455.

(38) Tian, L.; Ghosh, D.; Chen, W.; Pradhan, S.; Chang, X.; Chen, S. *Chemistry of Materials* **2009**, *21*, 2803.

(39) Zhou, J.; Booker, C.; Li, R.; Zhou, X.; Sham, T.-K.; Sun, X.; Ding, Z. *Journal of the American Chemical Society* **2007**, *129*, 744.

(40) Sun, Y.-P.; Zhou, B.; Lin, Y.; Wang, W.; Fernando, K. A. S.; Pathak, P.; Meziani, M. J.; Harruff, B. A.; Wang, X.; Wang, H.; Luo, P. G.; Yang, H.; Kose, M. E.; Chen, B.; Veca, L. M.; Xie, S.-Y. *Journal of the American Chemical Society* **2006**, *128*, 7756.

(41) Chan, W. C. W.; Nie, S. *Science* **1998**, *281*, 2016.

(42) Ebenstein, Y.; Mokari, T.; Banin, U. *Applied Physics Letters* **2002**, *80*, 4033.

A table of contents entry
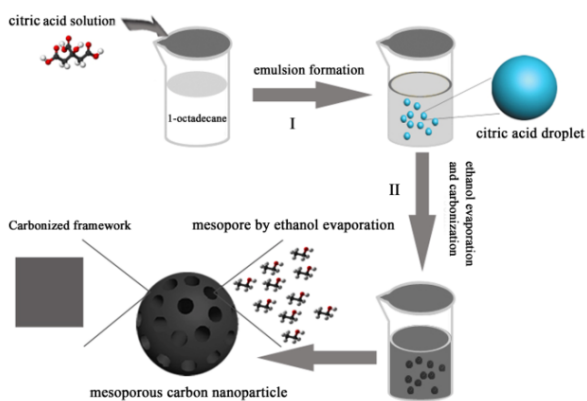
Hydrophilic mesoporous carbon nanoparticles have been synthesized by a precursor carbonization-in-solvent route, which displays multicolor and upconversion photoluminescence properties